

# Towards Aerodynamic Characteristics Investigation Based on Cartesian Methods for Low-Reynolds Number Flow Simulation

Daisuke Sasaki, Yuya Kojima, Daiki Iioka, Ryohei Serizawa and Shun Takahashi

**Abstract** Micro Aerial Vehicles (MAVs) are recently focused for various usage such as monitoring, photographing, and filming. One of the issues of MAVs is the limitation of operation time. An efficient configuration is required for MAVs, however, complex low-Reynolds number flows causes the difficulty. In this research, Cartesian-based CFD approach is applied to a flat plate, a NACA0012 airfoil, and a circular arc at low-Reynolds number flows to investigate the aerodynamic characteristics. Block-structured Cartesian mesh solver, Building-Cube Method, was capable to investigate the complicated flowfields at lower angles of attacks.

## 1 Introduction

Micro Air vehicles (MAVs) have been widely researched and developed in recent years for various purposes, such as the disaster monitoring and aerial photographs. The aerodynamic characteristics of MAVs is different from large passenger aircrafts because of low Reynolds number flows. Conventional airfoils such as NACA series, which are thick and streamlined shapes, generally produce low aerodynamic performance at low Reynolds number in MAVs flight regime. Instead, it is well-known that thin airfoils can often increase the aerodynamic performance by making use of laminar separation bubble at sharp leading-edge [1]. Therefore, the complicated flow phenomena needs to be precisely investigated through Computational Fluid Dynamics (CFD) and wind/water tunnel tests to improve aerodynamic performances [2, 3].

It is required to solve complicated flowfields precisely to obtain accurate aerodynamic performance at low Reynolds number conditions. Cartesian mesh is expected to solve such flowfields because it can prevent numerical vortex dissipation and maintain vortices. Building-Cube Method (BCM [4]) is a block-structured Cartesian mesh

---

D. Sasaki (✉) · Y. Kojima · D. Iioka  
Kanazawa Institute of Technology, 3-1 Yatsukaho, Hakusan, Japan  
e-mail: dsasaki@neptune.kanazawa-it.ac.jp

R. Serizawa · S. Takahashi  
Tokai University, 4-1-1 Kitakaname, Hiratsuka, Japan

CFD solver proposed for efficient parallel computation. The objective of the study is to conduct incompressible flow computations on various airfoils at different computational conditions to investigate the capabilities of BCM solver for low-Reynolds number flows. The computational models are a flat plate, a thick airfoil (NACA0012), and a circular arc, all of which have different flow characteristics.

## 2 Building-Cube Method

This study adopts block-structured Cartesian mesh solver, Building-Cube Method (BCM). The code employs incompressible Navier-Stokes equations. BCM simplifies pre-process, computation, and post-process. It is easy to generate mesh for a real-world complicated shape, and also to implement spatial higher-order accuracy scheme. BCM divides computational domain with many blocks, named Cubes, which are shown in Fig. 1. Equally-spaced Cartesian mesh, so-called Cells, are then filled in each Cube. Computational domain is composed of many Cubes with different size, but each Cube possess the same number of Cells regardless the Cube size. The method allocates a lot of small-size Cubes near the model where physical quantities change largely, thus dense mesh is only distributed to the vicinity of the model. Therefore, in the domain allocated with minimum cell, high spatial accuracy is maintained and also numerical vortex dissipation is prevented. This is advantage against complicated flowfields with separation bubble and large vortices around thin airfoil under low Reynolds number range. In addition, it can be easy to conduct parallel computation while maintaining parallel efficiency. Individual Cubes are computed independently, thus BCM needs to exchange physical quantities between the adjacent

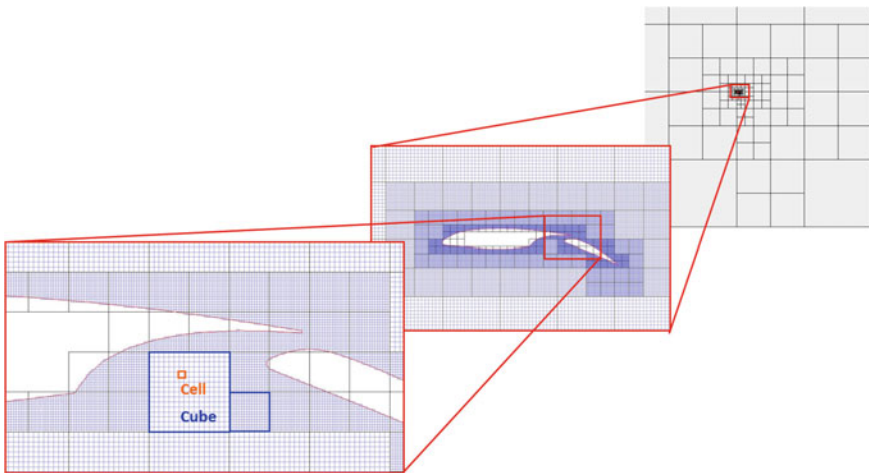
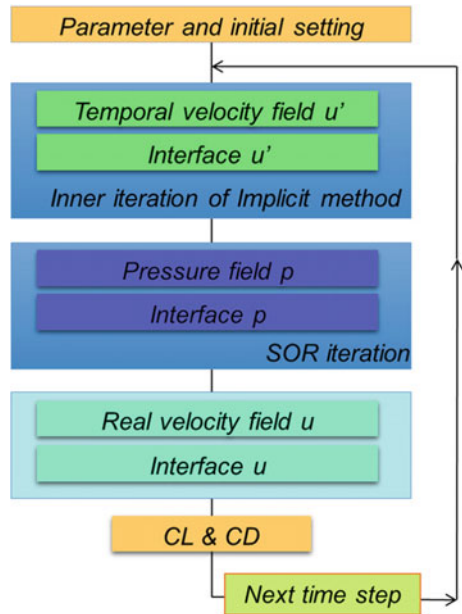


**Fig. 1** Cube allocation around multi-element airfoil (cube and cell)

**Fig. 2** Flowchart of fractional step method



Cubes during the computational process. In this computation, there are overlap area of 2 Cells between adjacent Cubes. Therefore, at the exchange process, Cubes of the same size can maintain the interpolation accuracy at Cube boundaries. However, in the case of Cubes of different size between adjacent Cubes, linear interpolation is conducted from small size Cube to large size one. Nearest neighbor interpolation is conducted from large size to small size Cubes.

The governing equations are equation of continuity and two- and three-dimensional Navier-Stokes equations. It is discretized on the collocated-mesh scheme. Pressure and velocity are located at cell-center, and additional quantity called contravariant velocity is located at cell-face. Navier-Stokes equation is integrated in time by fractional step method in Fig. 2. Adams-Bashforth explicit scheme is employed for convective and diffusive terms. The convective term is discretized using first-order accurate upwind difference scheme. Second-order accurate central difference scheme of second derivative is adopted for the diffusive term. Wall is treated as staircase representation. In this study, turbulent model is employed, and thus the inflow boundary condition is set as laminar flow.

### 3 Computational Model and Conditions

The target of the computation is 2% flat plate, NACA0012 airfoil, and circular arc as shown in Fig. 3, which were experimented by Kuroda et al. [2]. The mesh near the airfoil is also shown in the figure. The characteristic length is chord length  $c$ , and the

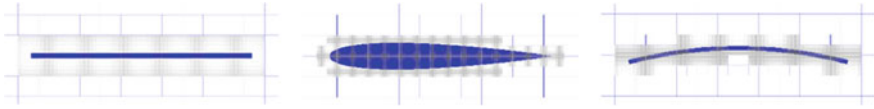


**Fig. 3** Computational model: flat plate (*left*), NACA0012 (*middle*), circular arc (*right*)

**Fig. 4** Computational domain

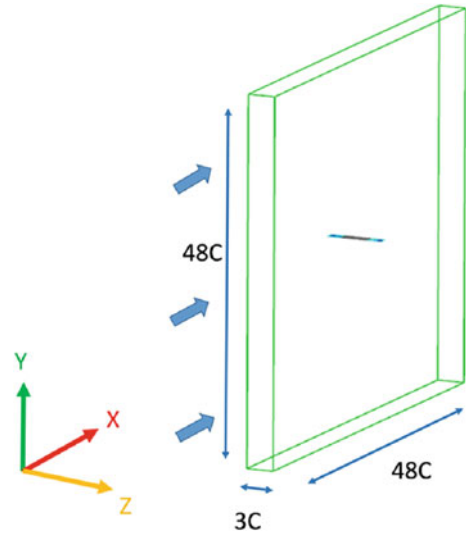


**Table 1** Computational conditions

Item	Flat plate	NACA0012	Circular arc
Reynolds number	$5.0 \times 10^3$	$2.8 \times 10^3$	$2.8 \times 10^3$
Min. cell size	$5.86 \times 10^{-3}$	$2.93 \times 10^{-3}$	$2.93 \times 10^{-3}$
Cells in a cube	$16^3$	$16^3$	$16^3$
Number of cubes	3,112	5,112	5,112
Number of cells	12,746,572	20,938,752	20,938,752

span length is three times of the chord length as shown in Fig. 4. Three-dimensional flow analysis is conducted and the periodic boundary condition is applied to both side of the wing tips. The inflow of computational domain is laminar flow. Table 1 describes computational condition.

## 4 Results and Discussion

### 4.1 Aerodynamic Computations of a Flat Plate

Two- and three-dimensional BCM incompressible solvers were applied to flows around a flat plate. The aerodynamic coefficients of the computations are plotted

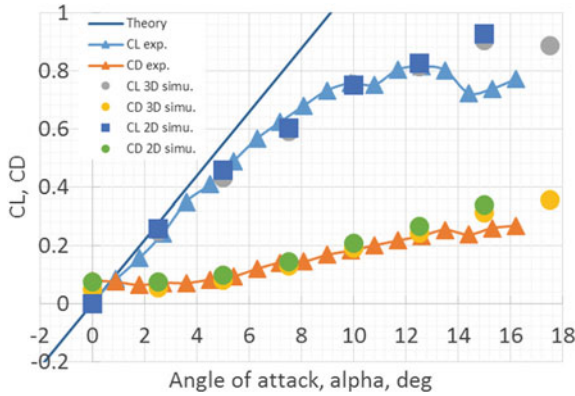


Fig. 5 Aerodynamic coefficient of a flat plate

in Fig. 5. Lift coefficients of two-dimensional and three-dimensional computations are well-matched with experiments except for the very high angles of attack, and the non-linearity of the  $C_L$  distribution are captured. However, drag coefficients show the discrepancy between two-dimensional and three-dimensional results. Two-dimensional results are relatively matched with experiments at lower angles of attack, while three-dimensional results are matched with experiments at large angles of attack. Freestream velocity distributions of 2.5 and 10° are shown in Figs. 6 and 7, respectively. At the low angle of attack (2.5°), the distributions are almost identical in

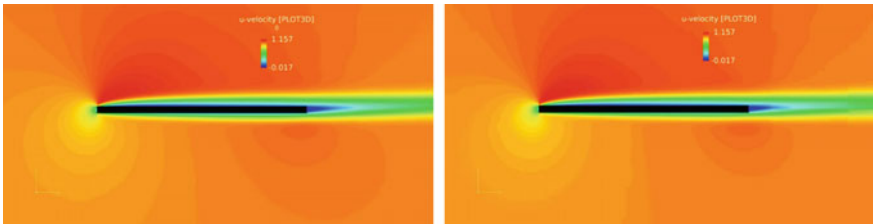


Fig. 6 Freestream velocity contours at 2.5°: 3D results (left), 2D results (right)

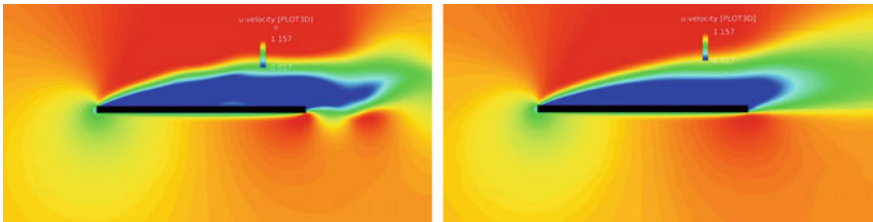
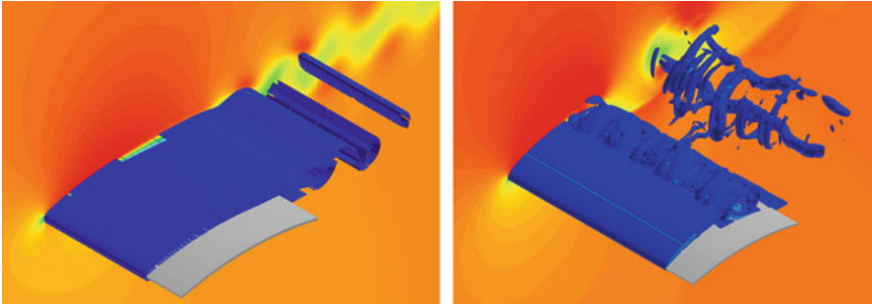


Fig. 7 Freestream velocity contours at 10°: 3D results (left), 2D results (right)



**Fig. 8** Vortex structures (iso-surface):. 2° (left), 10° (right)

two-dimensional and three-dimensional cases. However, the difference is observed at the wake region in Fig. 7. Figure 8 shows the vortex structure at 2 and 10°. It is obvious that the generated vortices are three-dimensional at higher angles of attack, thus three-dimensional computations agree well with experiments.

### 4.2 Aerodynamic Computations of NACA0012

Figure 9 shows the computational and experimental aerodynamic coefficients of NACA0012. Experimental results show the slight non-linearity of  $C_L$  distribution, while computational results show the linear relation with regard to angles of attacks.

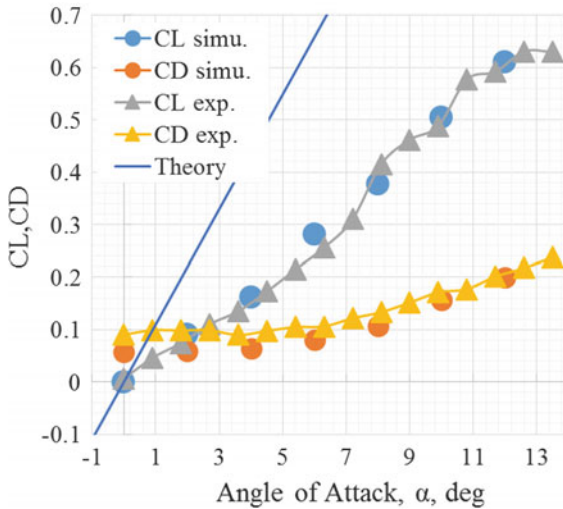


**Fig. 9** Aerodynamic coefficient of a NACA0012 airfoil

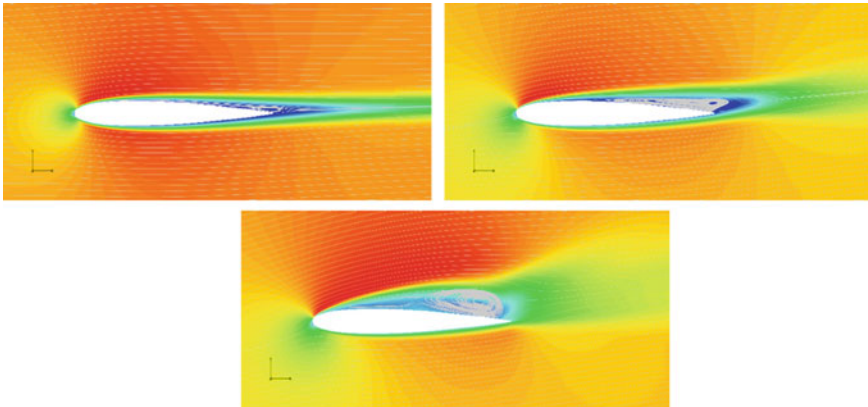


**Fig. 10** Freestream velocity contours around NACA0012 airfoil: 2° (*top left*), 6° (*top right*), 10° (*bottom*)

Freestream velocity contours with streamlines of NACA0012 airfoil are shown in Fig. 10. The separation location at 2° is close to the middle and the small separation vortex is formed. As the angle of attacks increases, the separation location moves forward and the separation vortex at the trailing edge becomes larger as appeared at 6°. The further increases of angle of attacks causes the separation location forward and the large separation vortex formed. Since the lift slope becomes lower at high angles of attacks, it is expected that the movement of separation location influences the non-linearity of  $C_L$  distribution.

### 4.3 Aerodynamic Computations of Circular Arc

Figure 11 shows the computed aerodynamic coefficients of a circular arc. Experimental results show the linear distribution of  $C_L$ , and computational results also show the similar trend that the linear relation with regard to angles of attacks is observed at lower angles of attacks. However, large discrepancy of computed  $C_L$  with experiments is observed at higher angles of attacks. Freestream velocity contours and streamlines in Fig. 12 shows that the separation occurs at near the maximum camber location at 2 and 6°, while the separation occurs at near the leading edge and the upper surface is covered with large vortices in computations. The strong unsteadiness is observed at 2°, but the unsteadiness gets weaker as the increase of angles of attacks to 6°. At the lower angles of attacks, the vortex is formed at near the trailing edge. On the other hand, separation location moves forward and the vortex covers the whole upper surface at higher angles of attacks, which leads the rapid increase of lift coefficient. It is possible the present computation at 10° or higher can not fully capture the flow features due to the lack of wake-region mesh resolution or the staircase

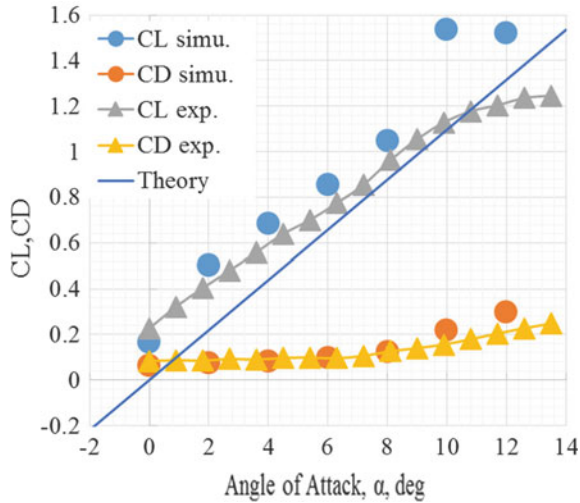


**Fig. 11** Aerodynamic coefficient of a circular arc

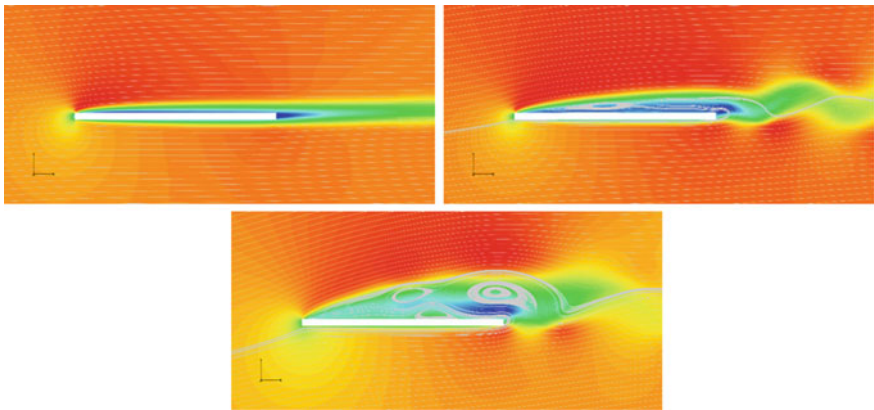


**Fig. 12** Freestream velocity contours around a circular arc.: 2° (top left), 6° (top right), 10° (bottom)

representation of curved surface or the employment of 1st order accurate scheme., which causes the difference with experimental values. Thus, further investigations of flowfields will be needed at higher angles of attacks.

### 5 Concluding Remarks

Cartesian-mesh based CFD solver, Building-Cube Method, was applied to various airfoils at low Reynolds number flows to investigate the aerodynamic characteristics. Three-dimensional flow computations are needed, where three-dimensional effects



of flow vortices can not be negligible. A conventional thick airfoil such as NACA0012 can not achieve good aerodynamic performance at the flow regime because of the separation vortex, while thin airfoil such as circular arc can produce higher aerodynamic performance because of the vortex formed. Thus, the present flow solver is capable to investigate the complicated flowfields at low Reynolds number region. However, more precise investigations are needed in terms of schemes and mesh density for high angles of attacks.

**Acknowledgements** Part of the work was carried out under the Collaborative Research Project of the Institute of Fluid Science, Tohoku University. Part of this research used computational resources of the HPCI system provided by Cyberscience Center at Tohoku University through the HPCI System Research Project (Project ID:hp140138 and hp150130).

## References

1. Alam, M., Sandham, N.D.: Direct numerical simulation of short laminar separation bubbles with turbulent reattachment. *J. Fluid Mech.* **410**, 1–28 (2000)
2. Kuroda, T., Okamoto M.: Unsteady aerodynamic forces measurements on oscillating airfoils with heaving and feathering motions at very low Reynolds Number. In: *Proceedings Asia-Pacific International Symposium on Aerospace Technology 2013*. Takamatsu (2013)
3. Iioka, D., Kojima, Y., Okamoto, M., Sasaki, D., Obayashi, S., Shimoyama, K.: Analysis of thin angular airfoils using block-structured Cartesian Mesh CFD. In: *Proceedings Asia-Pacific International Symposium on Aerospace Technology 2015*, (2015)
4. Sakai, R., Obayashi, S., Matsuo, K., Nakahashi, K.: Practical large-scale turbulent flow simulation using building-cube method. In: *Proceedings 45th Fluid Dynamics Conference/Aerospace Numerical Simulation Symposium 2013*, JSASS-2013-2116-A, Funahori (2013)